JOURNAL OF AIRCRAFT
Vol. 34, No. 5, September–October 1997

Helicopter Inverse Simulation Incorporating an Individual Blade Rotor Model

Stephen Rutherford* and Douglas G. Thomson†
University of Glasgow, Glasgow G12 8QQ, Scotland, United Kingdom

Inverse simulation is used to calculate the control displacements required for a modeled vehicle to perform a particular maneuver. As with all simulations, the usefulness of the technique depends on the validity of the mathematical model used. To incorporate the latest forms of helicopter model (individual blade models) in an inverse framework, it has been necessary to modify existing inverse techniques. Such a model is described in this paper along with an inverse algorithm capable of accommodating it. The resulting simulation is validated against flight data and comparisons are made with a more basic model. It is shown that the basic disk model compares well with the more comprehensive individual blade model until the severity of the maneuver is increased to encompass flight states where nonlinear aerodynamics effects are prevalent.

Nomenclature

h	= height of obstacle in pop-up maneuver
$[J]$	= Jacobian matrix
P, Q, R	= helicopter angular velocity components
R	= rotor radius
$\boldsymbol{r}$	= position vector
r, r_{elem}	= spanwise distance to blade element center from hub and hinge, respectively
s	= distance to obstacle in pop-up
t	= time
t_m	= time taken to complete pop-up maneuver
U, V, W	= translational velocity components of helicopter c.g.
$\boldsymbol{u}$	= control vector
$\boldsymbol{u}_{error}$	= control error vector
V_f	= helicopter flight velocity
$\boldsymbol{x}$	= state vector
x_e, y_e, z_e	= displacements relative to an Earth fixed inertial frame
$\boldsymbol{y}$	= output vector
$\boldsymbol{y}_{desired}$, $\boldsymbol{y}_{error}$	= desired and error output vectors
α	= blade element angle of attack
Δt	= maneuver discretization interval
θ_{twist}	= blade geometric twist
θ_0	= main rotor collective pitch angle
$\theta_{0_{tr}}$	= tail rotor collective pitch angle
θ_{1_s}, θ_{1_c}	= longitudinal and lateral cyclic pitch angles
ϕ, θ, ψ	= aircraft attitude angles

I. Introduction

THE conventional approach adopted in flight simulation is to calculate the response of a modeled vehicle to prescribed control inputs. This is achieved by integrating the differential equations of motion, allowing the vehicle's trajectory to be computed in response to a defined pilot control sequence. Interest in an alternative approach, known as inverse simulation, is growing. This form of simulation involves calculating the pilot inputs required for a modeled vehicle to fly a prescribed trajectory or maneuver. Inverse simulation is particularly useful in studies of flight involving precision maneuvering. At the University of Glasgow, applications have been related to helicopter flight dynamics and have included studies of safety during takeoff from off-shore platforms,[1] maneuverability in nap-of-the-Earth flight,[2] and workload while flying ADS-33 mission task elements.[3] Other researchers have applied this technique to control systems studies[4] and helicopter agility.[5]

The helicopter inverse simulation developed at Glasgow, Helinv,[6] makes use of a mathematical model known as HGS[7] (helicopter generic simulation), which describes a single main and tail rotor helicopter. This is a nonlinear model with seven degrees of freedom (the usual six body modes plus rotorspeed), and has what is termed a disk representation of the main and tail rotors. In this form of rotor model, elemental blade forces are calculated from simplified linear aerodynamic relationships and expressed as functions of azimuthal and radial position. The elemental forces are then integrated symbolically to give closed-loop expressions for the rotor forces and moments. Clearly, this type of model is limited as it is not possible to accommodate nonlinear aerodynamic properties such as Mach number variation, three-dimensional blade tip effects, or retreating blade stall, all of which have significant influence on the thrust generated by the rotor. Nonetheless, this model has provided useful and valid results[8] for a wide range of applications.

To further extend the range of applicability (allowing valid simulation at the extremes of the flight envelope) requires the development of a more comprehensive model. The natural progression is to a so-called individual blade model, where the disk representation of the rotor is replaced by individual models of each of its blades. Elemental blade forces are integrated numerically, allowing more accurate representation of the aerodynamic properties to be included. Another fundamental difference between the two models is that the rotor loads calculated by the disk model are in effect averaged for a complete revolution of all of the blades, i.e., a single steady value is computed over the period of rotation. This is in contrast to the individual blade model where the effect on the blade loads caused by the periodicity of their motion is fully captured, and as a consequence, the rotor forces calculated (which are subsequently applied to the body equations), are periodic. A model of this type, known as Hibrom[9] (helicopter individual blade rotor model), has been developed at Glasgow specifically for use in inverse simulation, the details of which are presented in Sec. III.

Received Aug. 6, 1996; revision received May 9, 1997; accepted for publication May 26, 1997.

*Postgraduate Researcher, Department of Aerospace Engineering.
†Lecturer in Flight Dynamics, Department of Aerospace Engineering. E-mail: d.g.thomson@aero.gla.ac.uk.

The numerical techniques associated with inverse simulation are still to a large extent under development.[10–12] The methods currently used fall into two categories: 1) those employing numerical differentiation and 2) those using numerical integration to solve the equations of motion. Using the numerical differentiation approach, the problem is discretized as all of the state variable rates are effectively calculated by numerical differencing. The differential equations of motion become algebraic and are readily solved for the control inputs. The alternative method uses repeated numerical integration of the equations of motion to determine the control displacements required to move the aircraft between closely spaced positional coordinates.

Helinv is an example of a differentiation-based inverse simulation. As discussed in the preceding text, there is a need to replace the disk model (HGS) originally implemented in Helinv with a more comprehensive individual blade model (Hibrom). Unfortunately, such a model does not lend itself well to implementation in an inverse form, at least as far as the numerical differentiation method is concerned. This is partly because of the structure of the model, but it is mainly because of the range of characteristic frequencies associated with the dynamics of the helicopter. The selection of an appropriate value for the time interval for the numerical differentiation becomes a difficult problem. The disk model only captures the low-frequency body modes of the aircraft, so that a relatively large time step can be used for differencing (possibly as large as 0.1 s) and, hence, rounding errors are usually avoided. This is not the case for the individual blade model where the higher frequency rotor dynamics require a much smaller time interval to evaluate their rates (typically less than 0.01 s). Experience has shown that this will lead to rounding error problems in the much more slowly moving body modes (for example, in a side-step maneuver the fuselage pitch attitude will change very little over a 0.01-s interval and, hence, the calculation of its rate may be prone to rounding error). Experience has also shown that these rounding errors eventually lead to failure of the inverse algorithm itself.

To implement an individual blade rotor model in an inverse sense, the alternative approach offered by the numerical integration technique is required. Unfortunately, this method can also exhibit unwanted features.[11,12] Work at Glasgow has solved many of the difficulties associated with this simulation technique[10] and a generic inverse simulation known as Genisa (generic inverse simulation algorithm) has been devised. The resulting methodology is presented in Sec. II along with a summary of the advances made during its development.

A crucial element of any simulation exercise is the validation of results. Section IV presents comparisons between an inverse simulation of a quick-hop maneuver and the actual maneuver flown by a Westland Lynx helicopter. Furthermore, a comparison of inverse simulation results between the two rotor models (individual blade and disk) shows the advantages to be gained in using an individual blade rotor model in terms of the significant rotor information that is derived.

II. Development of a Robust and Stable Generic Inverse Simulation Methodology

In all cases, the initial phase of any inverse simulation is the definition of the trajectory or maneuver that is to be flown. This acts as the input to the simulation, and a typical example of one such maneuver definition is now presented.

A. Maneuver Definition

Maneuvers are defined essentially as a series of positional coordinates (relative to an Earth fixed frame of reference), equally spaced in time $[x_e(t), y_e(t), z_e(t)]$. The helicopter's component velocities $[\dot{x}_e(t), \dot{y}_e(t), \dot{z}_e(t)]$ and accelerations $[\ddot{x}_e(t), \ddot{y}_e(t), \ddot{z}_e(t)]$ in the Earth fixed frame of reference are then obtained by differentiation. This ensures that the vehicle's c.g. follows the correct trajectory; however, it is still free to adopt an unspecified attitude. It is therefore necessary to prescribe one of the vehicle attitude angles [the heading angle $\psi(t)$ being the most convenient] to guarantee a realistic maneuver and vehicle response. Thus, the desired output vector $\boldsymbol{y}_{\mathrm{desired}}$ can be easily constructed using three Earth fixed displacements and headings:

$$\boldsymbol{y}_{\mathrm{desired}} = (x_e \quad y_e \quad z_e \quad \psi)^T \tag{1}$$

and is, in effect, the input to the inverse simulation.

As an example, consider the pop-up maneuver (Fig. 1), where it is assumed that the pilot's task is to clear an h over some distance s. A series of boundary conditions are applied to the altitude of the helicopter at the entry and exit of the maneuver. The simplest analytical function that satisfies these conditions is fifth-order polynomial:

$$z_e(t) = -h\left[6\left(\frac{t}{t_m}\right)^5 - 15\left(\frac{t}{t_m}\right)^4 + 10\left(\frac{t}{t_m}\right)^3\right] \tag{2}$$

where t_m is the time taken to complete the maneuver. To complete the description we assume that the pop-up performed at constant heading, i.e., $\psi(t) = 0$ and velocity V_f, and that there are no lateral excursions, i.e., the maneuver is longitudinal and performed in the $x_e - z_e$ plane, giving $y_e(t) = 0$. The longitudinal displacement $x_e(t)$ can be evaluated numerically by integrating

$$\dot{x}_e(t) = \sqrt{V_f^2 - \dot{z}_e(t)^2}$$

while the t_m can be calculated by specifying the total track distance s, then noting that

$$s = \int_0^{t_m} \dot{x}_e(t)\,\mathrm{d}t$$

In essence, the complete maneuver may be defined by specifying values for the parameters s, h, and V_f. The final simulation results are sensitive to the form of the maneuver applied as input. For example, Eq. (2) may be substituted for a seventh, ninth, or higher-order polynomial, simply by adding further constraints at the entry and exit points. The basic parameters s, h, and V_f will be satisfied in each case, but the profile will be quite different, particularly in the higher-order derivatives of the chosen function. The demanded accelerations are then different; hence, the control displacements required to provide them also differ. This approach may seem simplistic, but past experience[2] has shown that profiles such as that given in Eq. (2) provide realistic trajectories. A more structured rationale for selecting maneuver profiles based on quickness values calculated from ADS-33 mission task elements[13] has been suggested by Thomson and Bradley.[3]

This maneuver definition must now be applied to the helicopter model in such a way that the control displacements necessary to fly it are calculated. The scheme used by Rutherford and Thomson is presented in detail in Ref. 10, and for clarity this is now summarized.

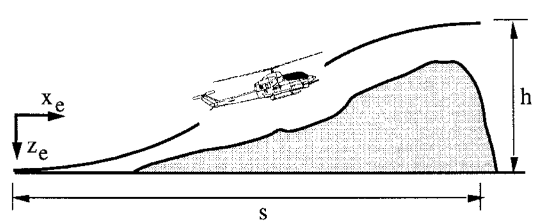

Fig. 1 Pop-up maneuver.

B. Genisa Algorithm

The nonlinear equations of motion may be expressed in the following form:

$$\dot{\boldsymbol{x}} = \boldsymbol{f}(\boldsymbol{x}, \boldsymbol{u}); \qquad \boldsymbol{x}(0) = \boldsymbol{x}_0$$

$$\boldsymbol{y} = \boldsymbol{g}(\boldsymbol{x})$$

For the helicopter we have

$$\boldsymbol{x} = [U \quad V \quad W \quad P \quad Q \quad R \quad \phi \quad \theta]^T$$

$$\boldsymbol{u} = [\theta_0 \quad \theta_{1_s} \quad \theta_{1_c} \quad \theta_{0_{tr}}]^T$$

The vector $\boldsymbol{y}$ is given by Eq. (1). In the context of an inverse simulation we require $\boldsymbol{u}$ to calculate for a given $\boldsymbol{y}$. The problem can be discretized into a series of time points t_k, at each of which there is $\boldsymbol{y}_{\text{desired}}(t_k)$ (as defined by the maneuver model), describing the position and heading of the helicopter. At the current time point $t = t_k$, the value of $\boldsymbol{x}(t_k)$ is known by integration of the state derivatives $\dot{\boldsymbol{x}}(t_{k-1})$ from the previous time point $t = t_{k-1}$. The influence of the control vector $\boldsymbol{u}(t_k)$ on $\dot{\boldsymbol{x}}(t_k)$ [and, consequently, $\boldsymbol{x}(t_{k+1})$ and $\boldsymbol{y}(t_{k+1})$] can be found by perturbing the current value. The problem is to effectively find a solution for $\boldsymbol{u}(t_k)$ that will produce a value of $\boldsymbol{y}(t_{k+1})$ equal to $\boldsymbol{y}_{\text{desired}}(t_{k+1})$. In simple terms, a guess is made as to what control inputs are required to move the helicopter from its current position (and heading) to that specified at the next time point in the maneuver definition. The equations of motion are then integrated in the usual manner, and the actual position produced using the estimated control displacements is calculated. The error between actual and desired position is then used as the basis for an iterative scheme to calculate exactly what control displacements are required to achieve the desired positional and heading change. The output error functions are solved over each interval, producing control time histories for the complete maneuver. This method has been used previously, by Gao and Hess[12] among others.

At a general time point (the mth estimate at the kth time point, $\dot{\boldsymbol{x}}(t_k)_m$ can be evaluated using $\boldsymbol{x}(t_k)$ and the current estimate for $\boldsymbol{u}(t_k)_m$:

$$\dot{\boldsymbol{x}}(t_k)_m = \boldsymbol{f}[\boldsymbol{x}(t_k), \boldsymbol{u}(t_k)_m] \tag{3}$$

This in turn can be integrated, using, for example, the method of Runge–Kutta,[14] to provide estimates of $\boldsymbol{x}(t_{k+1})_m$ and $\boldsymbol{y}(t_{k+1})_m$ at the next time point:

$$\boldsymbol{x}(t_{k+1})_m = \int_{t_k}^{t_{k+1}} \dot{\boldsymbol{x}}(t_k)_m \, \mathrm{d}t + \boldsymbol{x}(t_k)_m \tag{4}$$

$$\boldsymbol{y}(t_{k+1})_m = \boldsymbol{g}[\boldsymbol{x}(t_{k+1})_m] \tag{5}$$

An error function is defined as the difference between the latest estimate of the output vector $\boldsymbol{y}(t_{k+1})_m$ and the desired value $y_{\text{desired}}(t_{k-1})$:

$$\boldsymbol{y}_{\text{error}}(t_{k-1})_m = \boldsymbol{y}(t_{k+1})_m - \boldsymbol{y}_{\text{desired}}(t_{k+1}) \tag{6}$$

The conventional approach[12] is to seek the condition $\boldsymbol{y}_{\text{error}}(t_{k+1})_m = \boldsymbol{0}$, usually by employing a Newton–Rapson solver such as

$$\boldsymbol{u}(t_k)_{m+1} = \boldsymbol{u}(t_k)_m - [J]^{-1}\boldsymbol{y}_{\text{error}}(t_{k+1})_m \tag{7}$$

where $[J]$ describes the rate of change of the output vector with respect to the control vector. The details of the Jacobian formulation are given later in the text. The Genisa algorithm uses a modified form of this iteration:

$$\boldsymbol{u}(t_k)_{m+1} = \boldsymbol{u}(t_k)_m - \boldsymbol{u}_{\text{error}}(t_k)_m$$

which in contrast to Eq. (7) does not involve inverting the Jacobian explicitly. Instead, the control error vector is evaluated by solution of the linear system in Eq. (8) using LU factorization[14]:

$$[J]\boldsymbol{u}_{\text{error}}(t_k)_m = \boldsymbol{y}_{\text{error}}(t_{k+1})_m \tag{8}$$

This method, by avoiding matrix inversion, should be more accurate and stable for a wider range of Jacobians.

Assuming that the problem to be solved involves a vehicle with n controls flying a maneuver defined by n parameters and then for the mth estimate at the kth time point, the Jacobian is an $n \times n$ matrix, the entries of which, $j_{ij}(t_k)_m$ are evaluated by differentiating each of $\boldsymbol{y}_{\text{error}\,i}(t_{k+1})_m$ with respect to each of the elements of the control vector $u_j(t_k)_m$. The expression for determining a Jacobian element is thus

$$j_{ij}(t_k)_m = \frac{\partial \boldsymbol{y}_{\text{error}\,i}(t_{k+1})_m}{\partial u_j(t_k)_m}$$

If the desired output is defined in terms of displacements, then the Jacobian is

$$[J] = \begin{bmatrix} \dfrac{\partial x_e}{\partial \theta_0} & \dfrac{\partial x_e}{\partial \theta_{1s}} & \dfrac{\partial x_e}{\partial \theta_{1c}} & \dfrac{\partial x_e}{\partial \theta_{0\,\text{tr}}} \\ \dfrac{\partial y_e}{\partial \theta_0} & \cdot & \cdot & \cdot \\ \dfrac{\partial z_e}{\partial \theta_0} & \cdot & \cdot & \cdot \\ \dfrac{\partial \psi}{\partial \theta_0} & \cdot & \cdot & \dfrac{\partial \psi}{\partial \theta_{0\,\text{tr}}} \end{bmatrix}$$

Within the algorithm, there are no analytical expressions for $\boldsymbol{y}$, and so the elements of the Jacobian must be calculated numerically by central differencing, the general representation of which is in the following equation:

$$\frac{\partial \boldsymbol{y}_{\text{error}\,i}(t_{k+1})_m}{\partial u_j(t_k)_m} = \frac{\boldsymbol{y}_{\text{error}\,i}\{t_{k+1}[u_j(t_k) + \delta u_j(t_k)]\}_m - \boldsymbol{y}_{\text{error}\,i}\{t_{k+1}[u_j(t_k) - \delta u_j(t_k)]\}_m}{2\delta u_j(t_k)_m}$$

All n output elements must be calculated at positive and negative perturbations from their current estimates and, hence, Eqs. (3–6) must be used a further $2n$ times. This process is repeated at a series of consecutive, equally spaced points in time along the maneuver giving time histories for the controls.

C. Structural Differences Between Integration and Differentiation Methods

The most significant difference between the two types of solutions is the time taken to produce results: Genisa is typically an order of magnitude slower than Helinv, mainly because of the large number of numerical integrations that have to be performed. Although this is a major drawback of the integration approach, its main advantage lies in the algorithm structure. In the differentiation method the necessity to express the rates of change of state variables by numerical differentiation forces the vehicle equations of motion to become embedded within the main inverse algorithm. As a result, making major changes to the model (or indeed to the form of the output $y_{desired}$) can require significant restructuring of the algorithm. This is not the case in methods using the integration scheme where the model and algorithm can be expressed independently. This is primarily because the iteration minimizes the error in flight path variables that are not explicit in the equations of motion. The result of this is that modeling enhancements do not necessitate changes in the algorithm structure; indeed it is possible to simulate completely different vehicles simply by changing the mathematical model. Further, should an alternative set of input motion constraints be desirable, then it is a simple case to modify the error functions. It is for these reasons, and despite the greatly increased computational time required, that the integration based method is often favored.

D. Improving the Numerical Stability of Integration-Based Inverse Simulations

The stability of solutions generated using the integration method can be compromised if too small a calculation time step Δt is used.[15,16] As first noted by Lin et al.,[11] "when there is an uncontrolled state variable, the integration inverse method may be unstable for small time step." This can be demonstrated by considering inverse simulation using the HGS model with multiblade flapping dynamics. Because a conventional helicopter has only four controls and the model in question has 10 degrees of freedom, it is clear that there will be uncontrolled states. The Genisa simulation does show evidence of the phenomenon identified by Lin et al.,[11] the pop-up results in Fig. 2 (where $s = 200$ m, $h = 30$ m, and $V_f = 80$ kn), for example, were produced using a time step of 0.01 s. The small discretization interval has introduced unstable oscillations whose period matches the size of Δt. This result is typical of those observed in other inverse simulations of this type and is without doubt a serious drawback to the use of such techniques. In the case of systems that have a wide range of characteristic frequencies, such as the helicopter, these problems can be restrictive. Indeed, for a more sophisticated individual blade helicopter model to be utilized for inverse simulation, a solution to the problem of numerical stability with small time steps is essential.

It is shown in Sec. II.B, Eq. (6), that the iterative solution most often used in integration inverse algorithms is based upon minimizing the difference between the actual and desired helicopter position:

$$y - y_{desired} = 0 \tag{9}$$

where the output vector contains the elements x_e, y_e, z_e, and ψ. The rationale behind making this choice is that it is most convenient and natural to describe a maneuver in terms of these parameters. A simple alternative to this is that the error to be minimized is defined in terms of the aircraft's acceleration, i.e., y contains the elements $\ddot{x}_e$, $\ddot{y}_e$, $\ddot{z}_e$, and $\ddot{\psi}$. In the maneuver definition used to initiate the simulation, the desired accelerations are evaluated simply by differentiating the representative polynomials [Eq. (2), for example, is readily differentiated to give $\ddot{z}_e$, etc.]. The algorithm as described in Sec. II.B. is unchanged; that is, estimates of control displacements are made and the equations of motion are integrated between time points until Eq. (9) is satisfied.

This simple modification has the effect of eliminating the instabilities observed previously. Figure 3 shows controls calculated for the sample pop-up described earlier, again using a time step of 0.01 s. Direct comparison can then be made between Figs. 2 and 3, and it is evident that the instabilities associated with a small time increment have been eliminated, leaving only low-amplitude oscillations associated with blade flapping. It is apparent then that a simple modification has produced a significant improvement in the quality of the results. A complete explanation of why such a dramatic improvement is achieved is given by Rutherford and Thomson.[10] In summary, however, the underlying reason is that an error function associated with accelerations will have greater sensitivity to control displacements than will one associated with positional displacements. This has implications when using nu-

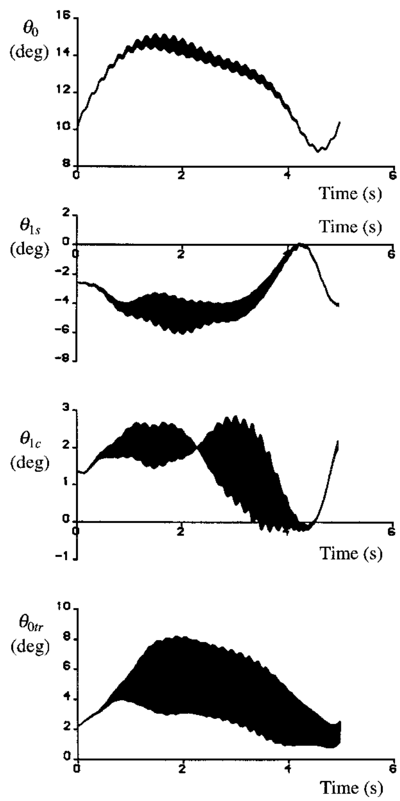

Fig. 2 Inverse simulation results using displacement error function (HGS model, Westland Lynx flying pop-up).

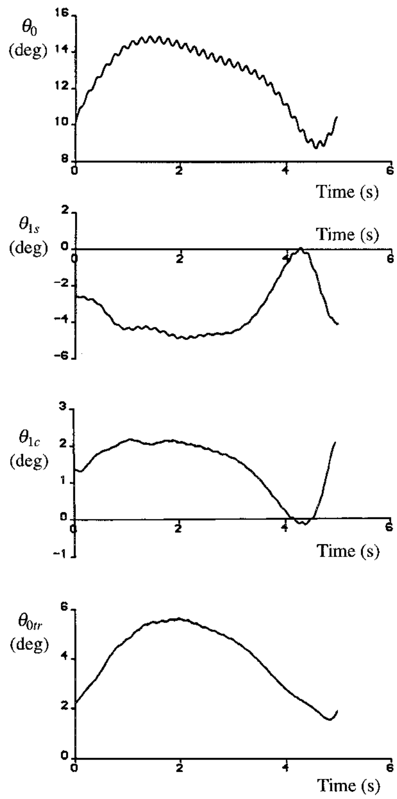

Fig. 3 Inverse simulation results using acceleration error function (HGS model, Westland Lynx flying pop-up).

merical differentiation to calculate the Jacobian. When using a very short time interval, the positional displacements caused by small perturbations in controls may be similar and very small, hence, leading to rounding errors in the differencing process. This may not be the case when using the more sensitive acceleration error vector, where even small positive and negative control displacements should provide distinct and differentiable function values.

It has been shown in this section that it is possible to obtain stable inverse simulation results using an inverse simulation technique, the structure of which is capable of accommodating a complex (individual blade) rotorcraft model. This combination is demonstrated in Sec. IV of this paper; however, it is first necessary to give some details of the individual blade helicopter mathematical model itself.

III. Development of an Individual Blade Rotorcraft Model, Hibrom

To successfully simulate a given aircraft requires calculation of the external forces and moments generated by each of the vehicle's components. For a helicopter, modeling the main rotor occupies the majority of effort as this is the most complex component. The forces and moments generated by a helicopter rotor are most conveniently estimated by use of blade element theory.[17] As already discussed in the context of helicopter simulation, there are two commonly adopted approaches: the disk model and the individual blade model. Blade element theory is used in both cases to calculate the rotor forces and moments, the primary difference being that simplifying assumptions regarding the aerodynamic properties of the blade elements are made in the disk model to allow analytical expressions to be derived. As will now be shown, this is not the case in an individual blade model where, as the integrations are performed numerically, it is possible to incorporate a more comprehensive representation of the aerodynamic and geometrical properties of the blade. The main modeling features of Hibrom are now summarized, a more detailed description is given by Rutherford and Thomson.[9]

A. Blade Dynamics

It is assumed that the main and tail rotor blades are fully rigid. This assumption has been found to be reasonable for simulating the flight mechanics of articulated rotor configurations,[18] but may result in poor prediction of the off-axis response of helicopters with semirigid rotors.[19] Lead/lag freedom has also been neglected.

B. Blade Aerodynamics

Aerodynamic data is for a NACA 0012 aerofoil[17] in the range of ± 18 deg, and compressibility effects have been included. The data has been blended with suitable low-speed data for the remainder of the 360-deg range to model the reversed flow region and fully stalled retreating blades. Dynamic stall effects have not been included.

C. Inflow Model

The dynamic inflow model of Peters and HaQuang[20] has been used. This model captures the effect of the rotor moments and the lag between application of the blade pitch and changes in the aerodynamic forces.

D. Blade Geometry

The spanwise variation of chord and geometric twist have been included in the blade elemental data.

E. Fuselage Aerodynamics

Look-up tables of force and moment coefficients generated from wind-tunnel tests of fuselage models have been used. The full 360-deg range of angle of attack and sideslip are accommodated.

So far in this paper, the development of an individual blade rotorcraft model and an inverse simulation methodology capable of accommodating it have been discussed. In the following section, sample results from this combination are given that illustrate both the validity of the model and the contrasting results from the more basic disk model implementation.

IV. Inverse Simulations Using an Individual Blade Rotorcraft Model

In this section, sample results from the use of the Genisa/Hibrom inverse simulation are compared with results from the Genisa/HGS simulation. The process of validating a mathematical model is essential before there can be confidence in the use of the simulation in practical applications. The results in the following section are therefore aimed at validating the Hibrom model.

A. Validation of Hibrom

The most common way of validating a mathematical model is to compare flight test results with those from the simulation. In simple terms, a standard control input may be applied to both vehicle and simulation, and the responses of both compared. In the context of an inverse simulation, it is possible to fly the vehicle and simulation through identical maneuvers, then compare both state and control time histories.[8]

For the current study, data from flight trials undertaken by the Defence Research Agency (DRA), Bedford, U.K., have been used. These trials were performed using a Westland Lynx helicopter, and the maneuver flown was the quick-hop. This maneuver is initiated from the hover, the pilot being instructed to translate forward to a new location some fixed distance away. Constant altitude and heading is to be maintained, and the aircraft is to be returned to the hover at the final position. Onboard instrumentation permits the vehicles states to be established throughout the maneuver. The pilot's control inputs are also measured allowing blade pitch angles to be obtained. The aircraft's position during the maneuver is recorded from ground-based measurements.

The flexibility of the integration inverse simulation technique is of particular value when validating mathematical models. It is possible to use the data measured during the trials as the error function for the simulation, in this case we have

$$y_{\text{desired}} = [\theta \quad \phi \quad \psi \quad \ddot{z}_e]^T$$

and with appropriate configurational data in the model it is possible to simulate the Lynx flying precisely the maneuver flown by the real aircraft.

Such a comparison is shown in Fig. 4, where the measured data from a quick-hop of a distance of 300 ft (91 m) has been used. From these plots it is apparent that the overall trends in each variable have been captured by the simulation, although the amplitude of some inputs do appear to be inaccurate (the initial pulse in longitudinal cyclic, for example). When considering where the modeling deficiencies lie, one must consider again the initial assumptions made in constructing the main rotor model. For example, the assumption that the blades are rigid may have a significant effect on the results. The torsional flexibility of the blade will superimpose pitch inputs in addition to those applied by the pilot, an effect that is not present in the mathematical model. Likewise, the modeled flapping dynamics and inflow may not completely replicate those of the real aircraft. A disk model is used for the tail rotor, and underprediction of the collective $\theta_{0_{tr}}$ is consistent with the observations of other authors.[21]

Clearly, the validation results shown here are insufficient to make a full assessment of the validity of the model, this is not the aim of the current research. However, while it is clear that the comparisons shown in Fig. 4 are inconclusive, the gross effects of the aircraft dynamics have been shown to be pre-

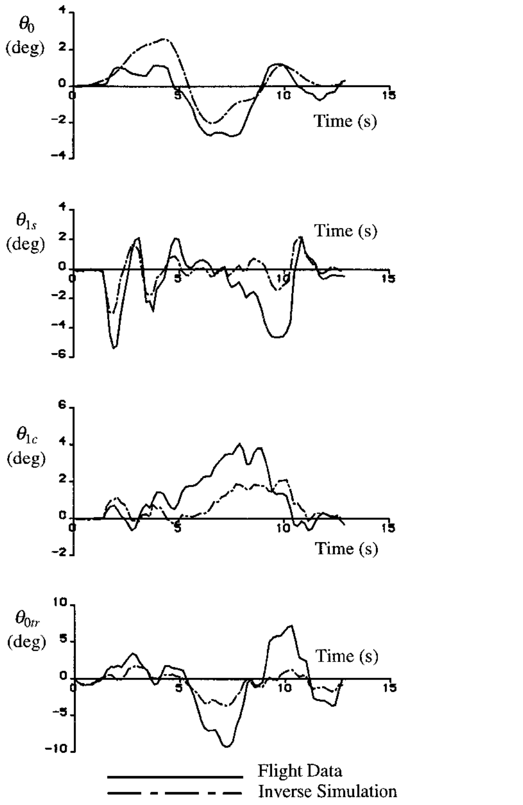

Fig. 4 Comparison of flight test and inverse simulation results for a Lynx helicopter flying a quick-hop maneuver.

dicted correctly. This and other similar results for different maneuvers gives sufficient confidence in the model to allow it to be used in range of flight mechanics applications.[22] The type of modeling enhancements required to improve the predictions will require little or no change to the inverse algorithm itself.

B. Comparison of Inverse Simulations Using Disk and Individual Blade Rotor Models

A comparison between inverse simulation results from the disk and individual blade models is of interest. One of the first issues to be decided upon is the choice of Δt. In using a disk model such as HGS in inverse simulation, the choice of a discretization interval is determined primarily by numerical stability. For inverse simulation using an individual blade rotor model, further consideration of the solution interval is required. This is because of the influence of the rotor dynamics. Too short a solution interval will result in poor prediction of the influence of control perturbations on the longer term dynamics of the aircraft as a result of transient effects. This can subsequently lead to failure of the algorithm. Consequently, an interval must be chosen that is sufficiently long to allow the transient dynamics to settle. Typically, this requires a time consistent with at least half a turn of the main rotor.

The oscillatory nature of the rotor forcing also means that the solution interval must coincide with an integer number of main rotor periods (a quarter turn for the four-bladed helicopter model used here). Note that this effect imposes the constraint of assuming constant rotorspeed on the model. For consistency, the same interval (0.086 s for the Lynx configuration) is used in both simulations.

A comparison of simulations is shown in Fig. 5 for the test pop-up maneuver described earlier. The comparison shows that both models predict very similar control displacements. This may seem like a disappointing result; however, it should be borne in mind that this is only a moderately severe maneuver and the linear assumptions made in the disk model will still be valid. The similarity of the HGS results to the supposedly more realistic individual blade model suggests that simpler disk models are applicable for the inverse simulation of moderately severe maneuvers. This assertion is confirmed when simulations from the individual blade and disk model are compared alongside flight data from the same moderately severe maneuver. The simulations give almost identical results, indicating a similar level of validity, and it can be deduced that the demanded maneuver has not drawn the individual blade model out to the edges of the flight envelope where its refined modeling should provide more accurate predictions.

Increasing the severity of the pop-up maneuver has a significant effect on the results. Figure 6 shows a comparison of results for the identical pop-up, but with the velocity increased to 85 kn. While HGS predicts control displacements that are very similar to those in Fig. 5, Hibrom's results are quite different. This is most evident in the discontinuous section of the lateral cyclic time history.

This can be explained by consideration of the fuselage pitch angle during the maneuver, (Fig. 7). It can be seen that during the exit phase of the maneuver, where the aircraft performs a push-over (in fact, the minimum load factor drops below 0.5 g) to clear the obstacle, the fuselage pitch attitude drops to around -20 deg. At this attitude and flight speed, the perpendicular blade velocity component becomes negative over a significant portion of the disk. The consequence of this is that on the retreating side of the disk, where the tangential velocity is small, we find large negative α. Figure 8 illustrates the variation of angle of attack of an inboard blade element (r/R = 0.25) during the pop-up maneuver as predicted by Hibrom. In both simulations, the modeled aerofoil section is the NACA 0012 profile; however, only the tabulated data used in Hibrom captures the stall characteristics of this section ($\alpha_{C_{l\max}} = \pm 15$ deg). It is clear from Fig. 8 that the stall is encountered on the retreating side of the disk throughout the pushover phase of the maneuver. The result of this is that a net rolling moment is generated, and the remedial action predicted by Hibrom is

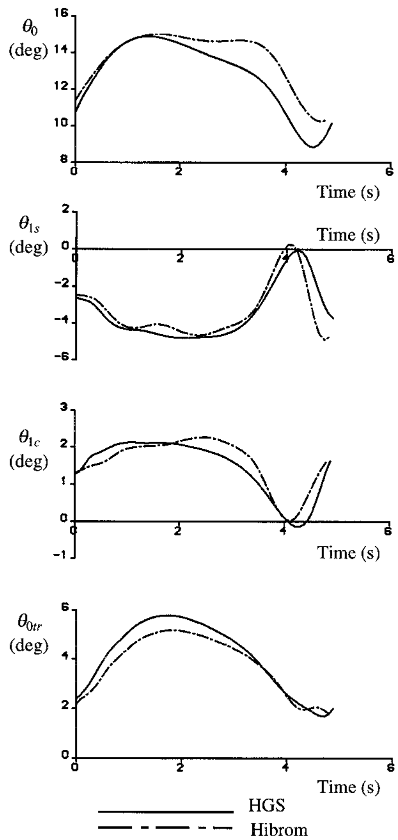

Fig. 5 Inverse simulation of a pop-up maneuver (s = 200 m, h = 25 m, and V_f = 80 kn) with data for Westland Lynx helicopter.

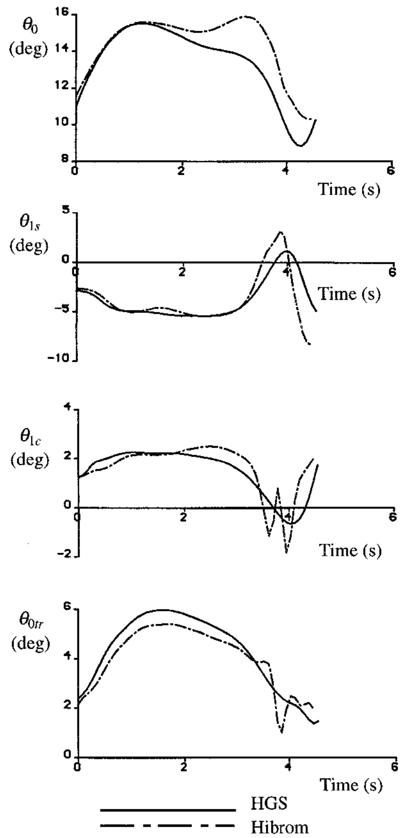

Fig. 6 Inverse simulation of a pop-up maneuver (s = 200 m, h = 25 m, and V_f = 85 kn) with data for Westland Lynx helicopter.

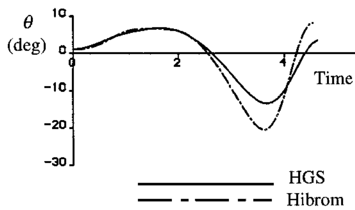

Fig. 7 Fuselage pitch angle during pop-up (85 kn) maneuver.

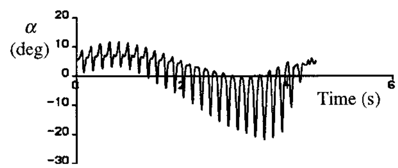

Fig. 8 Angle of attack of Hibrom inboard blade station during pop-up (85 kn).

a rapid input of lateral cyclic stick to counteract this moment. This effect is entirely missed by the HGS disk model because the stalling characteristics are not predicted by the linear representation of lift coefficient.

It can be argued that such large and rapid inputs are unlikely to be applied by a real pilot. In this case, a real pilot would be likely to feel the onset of the stall through vibration, and easeoff slightly during the pushover. From the results shown here, it is clear that the maneuver can be flown well within the control limits of the helicopter, but the low load factor in the pushover phase causes severe blade stalling, an important feature simply not captured by the disk model. In fact, as the speed of the helicopter through the maneuver is gradually increased (thereby increasing the severity of the maneuver), the individual blade model, Hibrom, predicts a limiting case of around 90 kn before severe blade stall causes failure of the algorithm (suggesting that this maneuver cannot be flown). On the other hand, the disk model, HGS, continues to predict solutions well beyond this velocity before control limits are breached. It can be concluded that the linear approximations made in the disk model are insufficient to accurately predict the aerodynamic loading of the rotor in severe flight states. It follows that if accurate results are required for maneuvers close to the extremities of the flight envelope, then an individual blade rotor model must be used.

V. Conclusions

From the research presented in this paper, the following conclusions can be drawn.

1) Helicopter individual blade models require integration methods for inverse simulation to accurately predict the wide range of characteristic frequencies.

2) The discretization interval should be expressed as a whole number of blade periods to capture the periodicity of the forces. For convenience, constant rotorspeed can be assumed to determine the calculation interval.

3) For improved numerical stability, the error function in the inverse algorithm should be based on accelerations rather than displacements.

4) As both disk and individual blade models have similar modeling features, both give similar results up to moderately severe flight states. As the severity of the demanded maneuver is increased, the nonlinear effects not simulated in the disk model become influential in the results from the individual blade model.

As the interest in inverse simulation grows, more effort must be applied to the associated numerical techniques to ensure that the algorithms do not impose constraints on the mathematical models used. If this form of simulation is to be more widely used it must be able to accommodate state-of-the-art mathematical models. A method of achieving this goal has been demonstrated in this paper.

Acknowledgments

This work was jointly funded by the United Kingdom Engineering and Physical Sciences Research Council and the Defence Research Agency. The authors wish to thank A. McCallum, M. Charlton, and G. D. Padfield of the DRA for their continuing support of this research.

References

[1]Thomson, D. G., Talbot, N., Taylor, C., Bradley, R., and Ablett, R., "An Investigation of Piloting Strategies for Engine Failures During Take-Off from Offshore Platforms," *Aeronautical Journal*, Vol. 99, No. 981, 1995, pp. 15–25.

[2]Thomson, D. G., and Bradley, R., "Modelling and Classification of Helicopter Combat Manoeuvres," *Proceedings of 17th ICAS Congress* (Stockholm, Sweden), International Council of the Aeronautical Sciences, 1990, pp. 1763–1773.

[3]Thomson, D. G., and Bradley, R., "The Contribution of Inverse Simulation to the Assessment of Helicopter Handling Qualities," *Proceedings of the 19th ICAS Conference* (Anaheim, CA), International Council of the Aeronautical Sciences, 1994, pp. 229–239 (Paper 7.3.2).

[4]McKillip, R. M., and Perri, T. A., "Helicopter Flight Control System Design and Evaluation for NOE Operations Using Controller Inversion Techniques," *Proceedings of the 45th Annual Forum of the American Helicopter Society*, American Helicopter Society, Alexandria, VA, 1989, pp. 669–679.

[5]Whalley, M. S., "Development and Evaluation of an Inverse Solution Technique for Studying Helicopter Maneuverability and Agility," NASA TM 102889, July 1991.

[6]Thomson, D. G., and Bradley, R., "Development and Verification of an Algorithm for Helicopter Inverse Simulation," *Vertica*, Vol. 14, No. 2, 1990, pp. 185–200.

[7]Thomson, D. G., "Development of a Generic Helicopter Mathematical Model for Application to Inverse Simulation," Dept. of Aerospace Engineering, Univ. of Glasgow, Internal Rept. 9216, Glasgow, Scotland, UK, 1992.

[8]Bradley, R., Padfield, G. D., Murray-Smith, D. J., and Thomson,

D. G., ''Validation of Helicopter Mathematical Models,'' *Transactions of the Institute of Measurement and Control*, Vol. 12, No. 4, 1990, pp. 186–196.

[9]Rutherford, S., and Thomson, D. G., ''Development of an Individual Blade Rotorcraft Model for Inverse Simulation of Severe Manoeuvring Flight,'' Dept. of Aerospace Engineering, Univ. of Glasgow, Internal Rept. 9604, Glasgow, Scotland, UK, 1996.

[10]Rutherford, S., and Thomson, D. G., ''Improved Methodology for Inverse Simulation,'' *Aeronautical Journal*, Vol. 100, No. 993, 1996, pp. 79–86.

[11]Lin, K. C., Lu, P., and Smith, M., ''The Numerical Errors in Inverse Simulation,'' AIAA Paper 93-3588, Aug. 1993.

[12]Gao, C., and Hess, R. A., ''Inverse Simulation of Large-Amplitude Aircraft Maneuvers,'' *Journal of Guidance, Control, and Dynamics*, Vol. 16, No. 4, 1993, pp. 733–737.

[13]Anon., ''Aeronautical Design Standard, Handling Qualities Requirements for Military Rotorcraft,'' ADS-33D, July 1994.

[14]Cheney, W., and Kincaid, D., *Numerical Mathematics and Computing*. 2nd ed., Brooks/Cole Publishing, Monterey, CA, 1985.

[15]Lin, K.-C., ''Comment on 'Generalized Technique for Inverse Simulation Applied to Aircraft Maneuvers,' '' *Journal of Guidance, Control, and Dynamics*, Vol. 16, No. 6, 1993, p. 1196.

[16]Hess, R. A., and Gao, C., ''Reply by the Authors to Kuo-Chi Lin,'' *Journal of Guidance, Control, and Dynamics*, Vol. 16, No. 6, 1993, pp. 1197, 1198.

[17]Prouty, R., *Helicopter Performance, Stability and Control*, Krieger, Malabar, FL, 1990.

[18]Turnour, S. R., and Celi, R., ''Modelling of Flexible Rotor Blades for Helicopter Flight Dynamics Applications,'' *Journal of the American Helicopter Society*, Vol. 41, No. 1, 1996, pp. 52–66.

[19]Mansur, M. H., Development and Validation of a Blade Element Mathematical Model for the AH-64A Apache Helicopter,'' NASA TM-108863, April 1995.

[20]Peters, D. A., and HaQuang, N., ''Dynamic Inflow for Practical Applications,'' *Journal of the American Helicopter Society*, TN, Vol. 33, No. 4, 1988, pp. 64–68.

[21]Padfield, G. D., and Du Val, R. W., ''Application Areas for Rotorcraft System Identification: Simulation Model Validation,'' AGARD-LS-178, 1991.

[22]Houston, S. S., ''Validation of a Blade-Element Helicopter Model for Large Amplitude Manoeuvres,'' *Aeronautical Journal*, Vol. 101, No. 1, 1997, pp. 1–7.